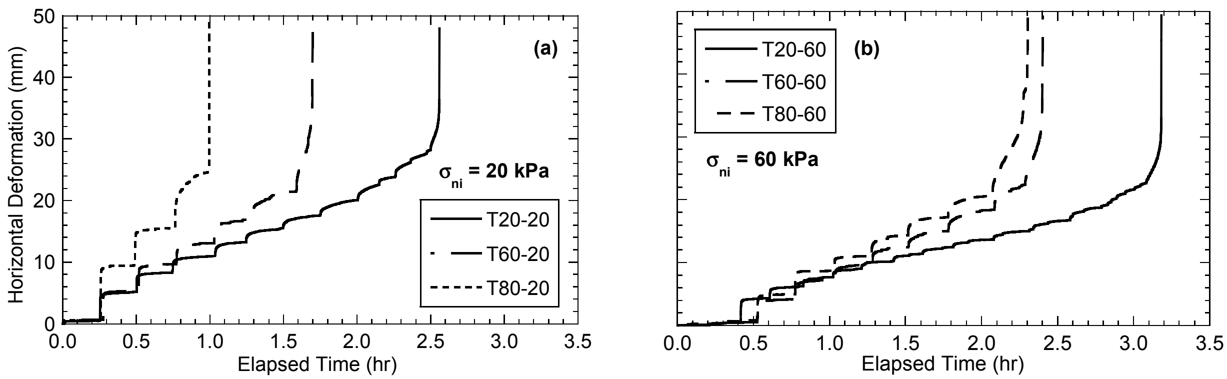

Figure 4. Temporal relationships of horizontal deformation as a function of temperature for geosynthetic clay liner shear tests conducted at (a) σ_{ni} = 20 kPa and (b) σ_{ni} = 60 kPa.

Relationships between total σ_n (i.e., reaction force + σ_{ni}) versus horizontal deformation are shown in Fig. 5a and 5b for experiments conducted at σ_{ni} = 20 kPa and σ_{ni} = 60 kPa, respectively. All data in Fig. 5 show an increase in total σ_n during initial horizontal deformation when shear stress was incrementally increased. Tensile stress within the needle-punched fibers increased with shear deformation, which generated a moment within the GCL and increased the reaction force. An increase in temperature reduced tensile strength of the reinforcement fibers, and this reduced tensile strength was believed to contribute to the decrease in reaction force and total normal stress for a given σ_{ni} (e.g., Fig. 5a). An increase in σ_{ni} also affects the reaction stress, and tests performed under σ_{ni} = 60 kPa experienced a smaller reaction force for a given temperature relative to tests conducted at σ_{ni} = 20 kPa. In all constant-stress tests, the reaction force reduced when reaching failure, which suggests that the developed reaction force and specimen rotation were related to tensile stress developed within the reinforcement fibers.

Relationships of net vertical displacement versus horizontal deformation are shown in Fig. 6a and 6b for experiments conducted at σ_{ni} = 40 kPa and σ_{ni} = 60 kPa, respectively. The net vertical deformation of a specimen was controlled by the reaction force placed at the back of the top shear platen (Fig. 1) and the ability for a specimen to rotate during shear. Thus, the tendency for specimens to compress or dilate during shear was based on σ_{ni} and test temperature. In experiments on T20-20 (Fig. 2c) and T20-40 (Fig. 6a), specimens exhibited dilative behavior at failure due to low σ_{ni} and temperature that allowed specimen rotation. In all other experiments, a higher applied σ_{ni} or higher temperature limited rotation within the GCL and net compression was observed both during the test and at failure. Temperature affected net compression via decreasing tensile strength of the reinforcement fibers, which reduced the tendency for rotation.

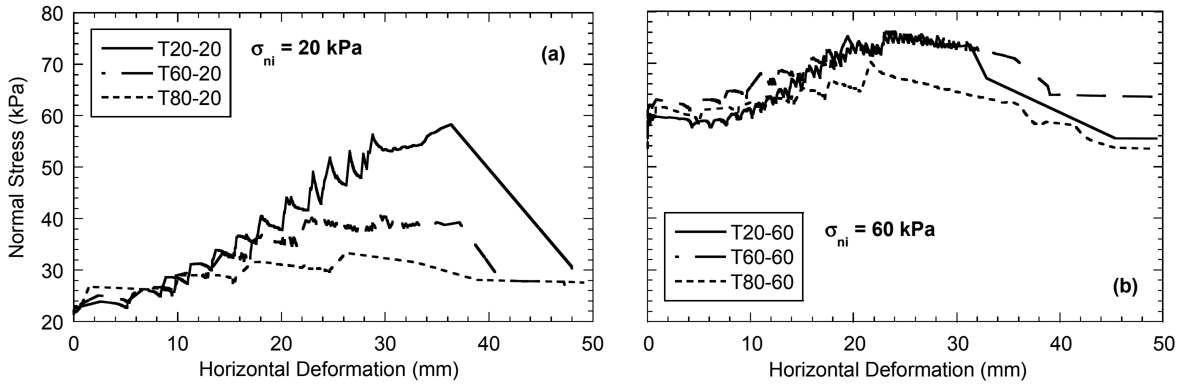

Figure 5. Relationships between total normal stress (initial dead weight + reaction) versus horizontal displacement for experiments conducted at(a) σ_{ni} = 20 kPa and (b) σ_{ni} = 60 kPa.

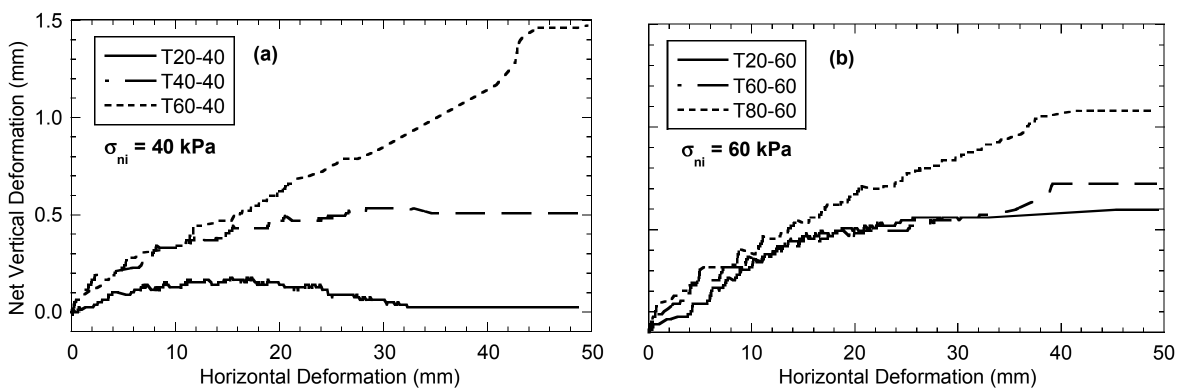

Figure 6. Relationships between net vertical deformation and horizontal deformation for experiments conducted at (a) σ_{ni} = 40 kPa and (b) σ_{ni} = 60 kPa

A compilation of shear-to-normal stress ratio at failure versus test temperature for all experiments conducted in this study is shown in Fig. 7. A general decreasing trend of shear-to-normal stress ratio at failure can be observed for all σ_{ni} with increasing temperature. This trend was attributed to reduced tensile strength of the needle-punched reinforcement fibers with increasing temperature, which decreased internal shear strength of the GCL.

CONCLUSIONS

Stress-controlled direct shear tests were performed on a needle-punched reinforced geosynthetic clay liner (GCL) at varying temperatures under three different applied normal stresses. Shear tests was performed in a state-of-the-art direct shear apparatus that allowed various combinations of shear and normal stresses to be applied to the GCL specimens while maintaining constant temperature. The following conclusions were drawn from the study.

- Shear deformation behavior of GCLs is dependent on the initial normal stress (σ_{ni}), whereby an increase in σ_{ni} yielded smaller horizontal deformation for a given applied shear stress due to higher internal shear strength.
- A reaction load measured at the back of the normal load plate was attributed to internal rotation of the GCL during shear via tensile stress within the reinforcement fibers. An increase in σ_{ni} reduced the reaction load via suppressing specimen rotation, and an increase in temperature reduced the reaction load via reducing tensile strength of the reinforcement fibers.
- Net vertical deformation of the GCL specimens was controlled by the amount of specimen rotation and corresponding change in total normal stress, both of which were affected by test temperature and σ_{ni}. An overall net compression during shear was measured for all specimens except for specimens tested under low normal stress and low temperature, which dilated slightly when approaching shear failure.
- An increase in test temperature led to increased horizontal deformation of GCLs via reducing tensile strength of the reinforcement fibers. Specimens tested at elevated temperatures reached failure at lower shear stresses, which yielded a decreasing trend between shear-to-normal stress ratio at failure and test temperature.

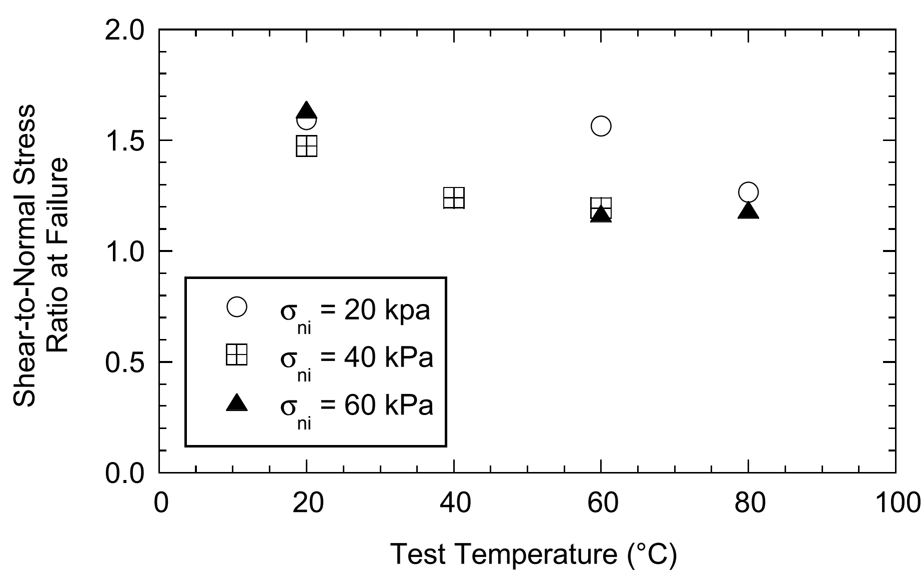

Figure 7. Compilation of shear-to-normal stress ratio at failure versus test temperature for all shear tests on geosynthetic clay liners conducted for this study.

ACKNOWLEGMENTS

Financial support for this study was provided by the Colloid Environmental Technologies Company (CETCO), Geosynthetic Research Institute (GRI), and Colorado State University (CSU). The opinions, findings, conclusions, or recommendations expressed herein are those of the authors and do not necessarily represent the views of CETCO, GRI, or CSU.

REFERENCES

Allen, J. M. and Fox, P. J. (2007). “Pyramid-tooth gripping surface for GCL shear testing. Geosynthetics”, *North American Geosynthetics Society*, Washington, DC, (CD-ROM).

Apiwantragoon, P., Benson, C. H., and Albright, W. H. (2015). “Field hydrology of water balance covers for waste containment”. *Journal of Geotechnical and Geoenvironmental Engineering*, 141(2), 1-20.

ASTM D4439 (2015). “Standard terminology for geosynthetics, Annual Book of ASTM Standards”, D4439-15a, *ASTM International*, West Conshohocken, PA, USA.

ASTM D 6072 (2015). “Standard Practice for Obtaining Samples of Geosynthetic Clay Liners.”, D4439-15a, *ASTM International*, West Conshohocken, PA, USA.

Chiu, P. and Fox, P. J. (2004). “Internal and interface shear strengths of unreinforced and needle-punched geosynthetic clay liners.” *Geosynthetics International*, 11(3), 176–199.

Farrag, K. (1998). “Development of an accelerated creep testing procedure for geosynthetics, part II: analysis”, *Geotech. Test. J.*, 21(1), 38-44.

Fox, P. and Stark, T. (2015). “State-of-the-art report: GCL shear strength and its measurement – ten-year update.” *Geosynthetics International*, 10-47.

Karademir, J. D., and Frost, J.D. (2014). “Micro-Scale Tensile Properties of Single Geotextile Polypropylene Filaments at Elevated Temperatures”, *Geotextiles and Geomembranes*, Elsevier, Vol. 42(3), DOI: 10.1016/j.geotexmem.2014.03.001.

Koerner, R. M., Soong, T.-Y., Koerner, G. R., and Gontar, A. (2001). “Creep testing and data extrapolation of reinforced GCLs”, *Geotextiles and* Geomembranes, 19(7), 413–425.

Mesri, G., and R. E. Olson. (1970). “Shear strength of montmorillonite", *Geotechnique*”, 20(3): 261-270.

Müller, W., Jakob, I., Seeger, S., and Tatzky-Gerth, R. (2008). “Long-term shear strength of geosynthetic clay liners”, *Geotextiles and Geomembranes*, 26(2), 130-144.

Stark, T. D. and Eid, H. T. (1996). “Shear behavior of reinforced geosynthetic clay liners.” *Geosynthetics International*, 3(6), 771–786.

Stark, T. D., Martin, J. W., Gerbasi, G. T., Thalhamer, T. and Gortner, R. E. (2012). “Aluminum waste reaction indicators in a municipal solid waste landfill”. *Journal of Geotechnical and Geoenvironmental Engineering*, 138(3), 252–261.

Steemson, M.L., Smith, M.E., 2009. “The development of nickel laterite heap leach projects”. In: *ALTA 2009 Nickel/Cobalt Conference*, May 25–30, Perth, Australia.

Thiel, R., and Smith, M.E. (2004). “State of the practice review of heap leach pad design issues”. *Geotextiles and Geomembranes*, 22 (6), 555–568.

Yesiller, N., Hanson, J. L., and Yee, E. H. (2015). “Waste heat generation: a comprehensive review”. *Waste Management*, 42, 116-179.

Zanzinger, H. and Saathoff, F. (2012). “Long-term internal shear strength of a reinforced GCL based on shear creep rupture tests”, *Geotextiles and Geomembranes*, 33, 43–50.

Numerical Evaluation of Boundary Effects on the Interaction between Geosynthetic Reinforcement and Backfill

Yan Jiang[1]; Jie Han[2]; Jorge G. Zornberg[3]; Dov Leshchinsky[4]; Barry R. Christopher[5]; and Burak F. Tanyu[6]

[1]Univ. of Kansas, Lawrence, KS 66045. E-mail: yan.jiang.geo@gmail.com
[2]Univ. of Kansas, Lawrence, KS 66045. E-mail: jiehan@ku.edu
[3]Univ. of Texas at Austin, Austin, TX 78712. E-mail: zornberg@mail.utexas.edu
[4]ADAMA Engineering, Inc., Clackamas, OR 97015. adama@geoprograms.com
[5]Independent Consultant, Roswell, GA 30075. E-mail: barryc325@aol.com
[6]George Mason Univ., Fairfax, VA 22030. E-mail: btanyu@gmu.edu

Abstract

Geosynthetics have been extensively used to reinforce soil structures, such as embankments, slopes, walls, foundations and roads. Proper evaluation of the interaction between geosynthetic reinforcement and backfill is important to understand the mechanisms of geosynthetic-reinforced soil (GRS) structures. Pullout tests have proven to be an effective way to study such interaction. In a pullout test, a geosynthetic reinforcement layer is buried in backfill within a test box. Vertical pressure is applied on top of the backfill to simulate the normal stress on top of the geosynthetic reinforcement in a GRS structure. The geosynthetic reinforcement is then pulled out from the backfill through an opening in the front wall of the box. The pullout test results are influenced by boundary conditions due to the thickness of the backfill, as well as the roughness of the interface between the backfill and the walls of the pullout box. This paper discusses the results of a numerical study performed to investigate the boundary effect on pullout test results. A two-dimensional numerical simulation was conducted using a finite differential method program, FLAC, using the Mohr-Coulomb model to describe the behavior of the backfill. The geosynthetic reinforcement was modeled as a linearly elastic and perfectly plastic material. The numerical model was calibrated and verified against pullout tests of geogrids. Boundary conditions, such as backfill thickness, and the roughness between the bottom of the backfill and the wall of the pullout box, and how these affect pullout test results are analyzed and discussed. The numerical results show that the pullout forces at the large pullout displacement calculated from the numerical simulation with the fixed bottom were closer to the measured pullout forces than those with the free bottom.

INTRODUCTION

Geosynthetics have been extensively used to reinforce soil structures such as embankments, slopes, walls, foundations and roads. The behavior of the interaction between geosynthetic reinforcement and backfill is important to understand the mechanisms of geosynthetic-reinforced soil (GRS) structures. Pullout tests have been reported to provide an effective way to study the interaction between geosynthetic reinforcement and backfill (e.g., Palmeira and Milligan 1989, Sugimoto et al. 2001, Moraci and Recalcati 2006, Abdi and Zandieh 2014, Wang et al. 2016). Although the pullout boxes used in these studies have generally met the boundary requirements based on ASTM D6706, they have involved a wide range of dimensions. The boundary effect on pullout test results has not been fully studied.

In this study, a numerical study was performed to investigate the boundary effects on pullout test results. A two-dimensional numerical simulation was conducted using a finite difference method program, FLAC, using the Mohr-Coulomb (MC) model to describe the behavior of the backfill. The geosynthetic reinforcement was modeled as a linearly elastic and perfectly plastic material. The numerical model was calibrated and verified against pullout tests of geogrids. Boundary conditions, such as the thickness of backfill, and the roughness between the backfill and the wall of the pullout box, and how these affect pullout test results are analyzed and discussed.

NUMERICAL MODEL

In support of this numerical investigation, pullout tests were performed on a uniaxial high-density polyethylene geogrid using three different confining pressures. The pullout box is 1.5 m long, 0.6 m wide and 0.6 m high. The details of this pullout box can be found in Mehari et al. (2016) and Jiang (2016). The backfill used in the pullout tests was an aggregate used in the construction of a mechanically stabilized earth (MSE) wall (Jiang et al. 2015 and 2016). Two separate layers of backfill were placed and compacted by a pneumatic hammer and the total thickness of backfill after compaction in the pullout box was 0.3 m. The length of the geogrid layer (excluding the width of sleeves) buried in the backfill was 1.2 m. Normal pressure was applied through an air bag. The geogrid layer was pulled out at a controlled displacement rate of approximately 1 mm/min. In addition, triaxial compression tests and a tensile test were performed to determine the properties of the aggregate and the geogrid, respectively, to be used in the numerical simulations.

A two-dimensional numerical model was developed to simulate the pullout tests. Figure 1 shows the mesh of the numerical model. The numerical model included a 1.5 m (length) by 0.3 m (thickness) backfill, and a 1.2 m long geogrid layer placed in the middle of the backfill. The left and right sides of the numerical model were fixed in the horizontal direction, but were allowed to move freely in the vertical direction. The bottom of the numerical model was fixed in the vertical direction but moved freely in the horizontal direction (referred to as a free bottom) to simulate the fully smooth bottom of the pullout box. A uniform normal pressure was applied on top of the numerical model to simulate the confining stress.

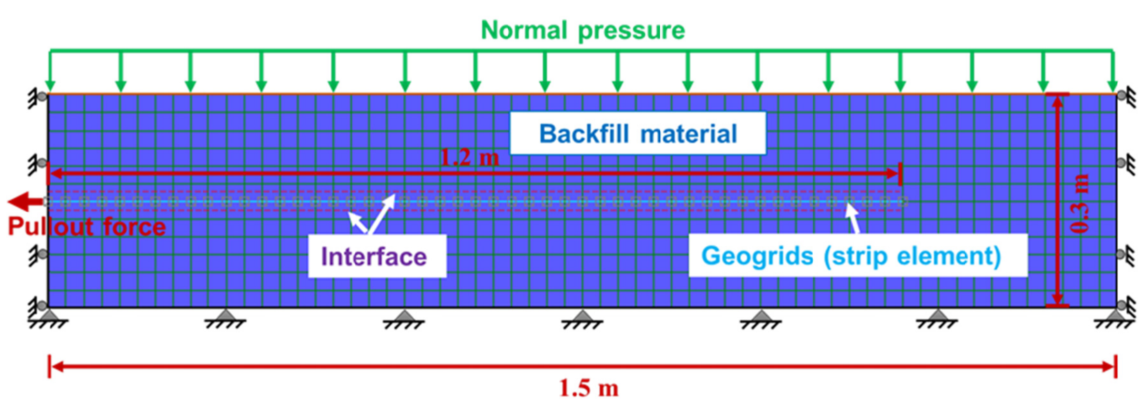

Figure 1. Mesh of numerical model

The backfill was modeled as a linearly elastic and perfectly plastic material with the Mohr-Coulomb failure criterion. This soil constitutive model has already been successfully employed to simulate the behavior of backfill in pullout tests (e.g., Abdi and Zandieh 2014). The parameters for the backfill used in the numerical simulation are summarized in Table 1. Figure 2 shows the comparison between measured and numerically calculated results of the triaxial tests. As seen in Figure 2, results from the numerical simulation using the MC model showed a reasonable agreement with those from the triaxial tests. It should be pointed out that the friction angle in the plane strain condition was used in the numerical simulation of pullout tests since the numerical simulation involves a plane strain condition. The following correlation recommended by Kulhawy and Mayne (1990) for cohesionless soils was used to convert the friction angle from triaxial compression tests to the friction angle in the plane strain condition: $\phi_s = 1.12\phi_{tc} = 1.12\times 47° = 52°$, where ϕ_s = the friction angle in the plane strain condition and ϕ_{tc} = the friction angle from triaxial compression tests.

Table 1. Parameters for backfill

Material	Constitutive model	Unit weight (kN/m^3)	Young's modulus (MPa)	Poisson's ratio	Cohesion (kPa)	Friction angle (°)	Dilation angle (°)
Backfill	Mohr-Coulomb	17.2	20	0.2	0	52	8

The numerical simulation involved applying a load to the front of the geogrid to simulate the pullout force during testing. The geogrid layer was modeled as a linearly elastic and perfectly plastic strip element. The properties of the geogrid are summarized in Table 2. The interface properties between the geogrid layer and the backfill were incorporated in the strip element. Table 2 also provides the interface properties between the geogrid layer and the backfill. Among these properties is the interface cohesion, which was assumed to be zero because the backfill was an angular granular material. An interface friction angle of 40° was used, which results from using the equation $\tan\phi'_{\text{int}} = c_r \cdot \tan\phi$, where $c_r = 0.67$ = reduction factor, and $\phi = 52°$ = friction angle of the backfill in a plane strain condition. The shear stiffness between the geogrid and the aggregate was calibrated by matching the curve from the numerical simulation with that from the pullout test under a normal pressure of 43.4 kPa, as shown in Figure 3. The numerical model was also verified by comparing the results calculated from the numerical simulation with those measured by the pullout tests at two other confining stresses.

NUMERICAL RESULTS

Figure 3 shows a comparison between the experimental results from the pullout tests and the numerical calculations. The numerical calculations showed good agreement with those measured from the pullout tests. Both the measured and calculated results show that the pullout force increases when the geogrid layer is pulled out, but the rate of this increase gradually decreases. Eventually, the pullout force becomes constant, indicating that the geogrid-backfill interface has yielded. In addition, an increase in the confining stress results in an increase in the pullout force. Overall, the curves between the pullout force and the displacement of the geogrid layer showed a hyperbolic trend.

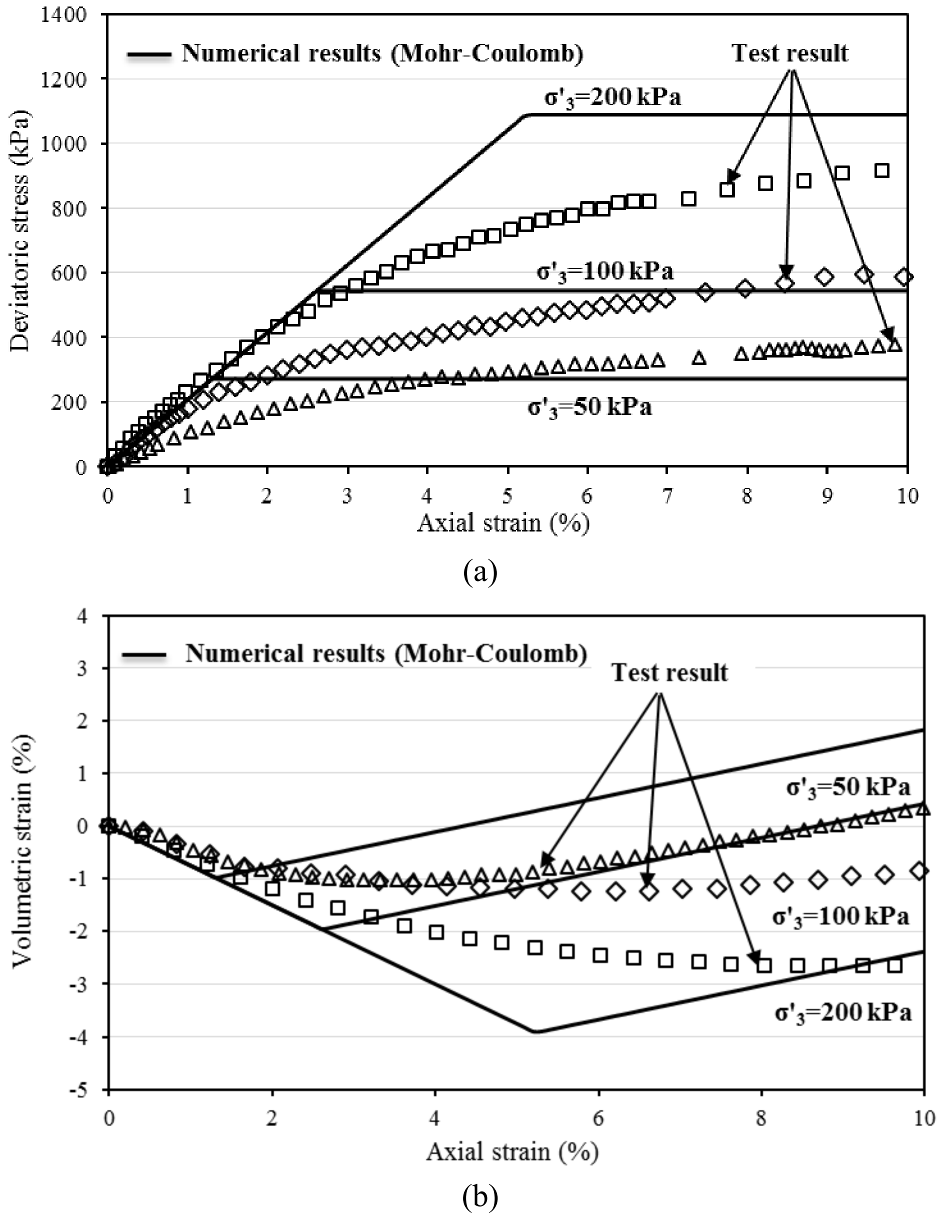

Figure 2. Comparison between measured and numerically calculated triaxial test results: (a) stress-strain relationship; (b) volumetric strain-axial strain relationship

Table 2. Parameters for geogrid and geogrid-backfill interface

Parameters	unit	Values
Secant stiffness, J	kN/m	820
Yield strength	kN/m	144
Tensile failure strain	%	20
Interface cohesion, c_{inter}	kN/m	0
Friction angle of interface, ϕ	°	40
Shear stiffness, k_s	kN/m/m	6500

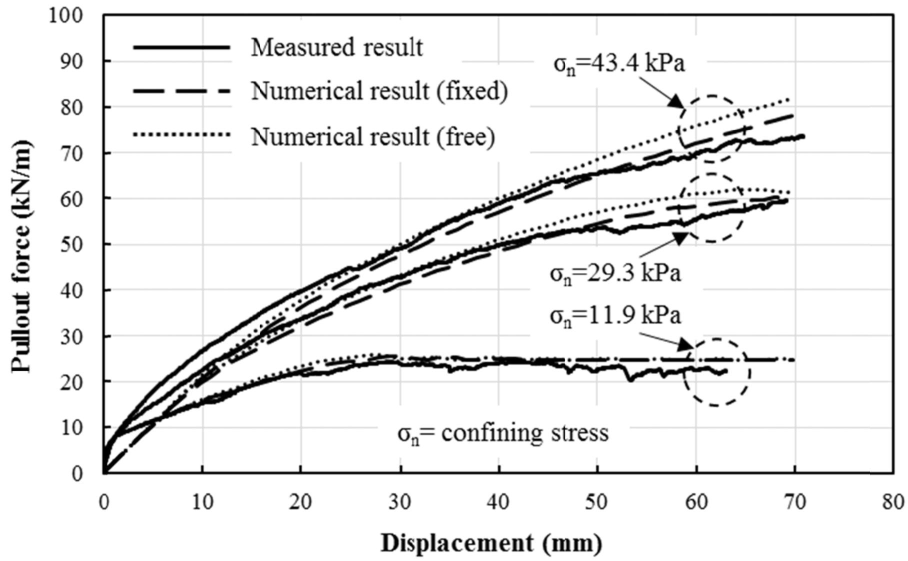

Figure 3. Comparison between measured and numerically calculated pullout test results

In the pullout tests, a layer of geotextile was installed at the bottom of the pullout box to provide a relatively smooth interface between the bottom of the backfill and the wall of the pullout box and reduce the influence of the interface roughness. In fact, the interface at the bottom of the backfill and the wall of the pullout box was not fully smooth, but friction developed between the backfill and the pullout box when the geogrid layer was pulled out. In the numerical simulation, the free bottom boundary condition was assumed to simulate an extremely smooth interface. Therefore, the free bottom boundary condition could not represent the actual friction between the bottom of the backfill and the wall of the pullout box. To simply consider the actual boundary at the bottom of the backfill in the numerical simulation, another case, with the bottom of the backfill fixed in both vertical and horizontal directions (referred to as a fixed bottom), was performed to simulate an extremely rough interface. The actual boundary condition should fall between these two extreme conditions. Figure 3 shows that the pullout forces calculated numerically with the fixed bottom were larger than those obtained with the free bottom. This influence of the interface roughness between the backfill and the wall of the pullout box became negligible when the confining stress was reduced to 11.9 kPa. Overall, the pullout forces calculated from the numerical simulation at the large pullout displacement with the fixed bottom were closer to the measured pullout forces than those with the free bottom.

An additional consideration is the thickness of the backfill in the pullout tests, which was 0.3 m. Although this thickness met the minimum value required by ASTM D6706, it can be expected that this small thickness had an influence on the pullout test results, especially given the rough interface between the bottom of the backfill and the wall of the pullout box. It is, therefore, of interest to understand the influence of the backfill thickness on the pullout test results. To investigate this influence, a larger thickness of backfill was numerically simulated. Specifically, the thickness of the backfill was increased to 0.6 m. The fixed and free bottom conditions were also considered in these simulations. Figure 4 shows the influence of the backfill thickness on the pullout test results. As seen in Figure 4, the pullout forces calculated numerically using the 0.6-m thick backfill were lower than those obtained with the 0.3-m thick backfill. However, the influence of the backfill thickness became negligible when the confining stress was reduced to